Power Parameter Analysis in the Electrochemical Graphite Exfoliation for Graphene Fabrication

Nur Afifah Muthmainnah
Department of Physics, Faculty of Mathematics and Science, Sebelas Maret University, Surakarta, Indonesia
nurafifahm30@student.uns.ac.id

Hendri Widiyandari
Department of Physics, Faculty of Mathematics and Science, Sebelas Maret University, Surakarta, Indonesia | Centre of Excellence for Electrical Energy Storage Technology, Sebelas Maret University, Indonesia
hendriwidiyandari@staff.uns.ac.id

Lita Rahmasari
Department of Physics Education, Faculty of Teacher Training and Education, Sebelas Maret University, Surakarta, Indonesia
lita@staff.uns.ac.id

Yulianto Agung Rezeki
Department of Physics Education, Faculty of Teacher Training and Education, Sebelas Maret University, Surakarta Indonesia
yarezeki@staff.uns.ac.id

Andita Nataria Fitri Ganda
Department of Mechanical Engineering, State University of Surabaya, Indonesia
anditaganda@unesa.ac.id

Suriani Abu Bakar
Nanotechnology Research Centre, Faculty of Science and Mathematics, Sultan Idris Education University, Malaysia
suriani@fsmt.upsi.edu.my

Sri Budiawanti
Department of Physics Education, Faculty of Teacher Training and Education, Sebelas Maret University, Surakarta Indonesia
sribudiawanti@staff.uns.ac.id

Anif Jamaluddin
Department of Physics Education, Faculty of Teacher Training and Education, Sebelas Maret University, Surakarta, Indonesia | Centre of Excellence for Electrical Energy Storage Technology, Sebelas Maret University, Indonesia
elhanif@staff.uns.ac.id (corresponding author)

Received: 29 January 2025 | Revised: 26 April 2025 | Accepted: 8 May 2025

 DOI: https://doi.org/10.48084/etasr.10360

ABSTRACT

Electrochemical exfoliation is considered an essential method for the rapid production of graphene in both high quality and quantity. This study investigates the electrochemical exfoliation of graphite rods, specifically the impact of the power variations in a Direct Current (DC) source on the quality of graphene. Furthermore, Scanning Electron Microscope-Energy Dispersive X-Ray (SEM-EDX) is employed to analyze the morphology and elemental composition. In addition, Fourier Transform Infrared (FTIR) spectroscopy is utilized to determine the functional groups of graphene. The defect of graphite is observed with Raman spectroscopy. The SEM results suggest that graphene layers are formed in all the power variations. Graphene at 98 W (G98) exhibits a wrinkle and cluttered surface compared to graphene at 70 W (G70) and graphene at 84 W (G84). Based on the FTIR results, the highest peak of C=O bond appeared in G70, while sharp peaks indicating O-H bonds are observed in G84 and G98. Furthermore, the power analysis is a critical factor affecting graphene mass production, with higher power levels resulting in higher graphene yield, but lower graphene quality by reducing the carbon (C) content and increasing Oxygen (O) content. This exploration contributes to advancing the understanding of the electrochemical exfoliation process, offering insights into optimizing the power parameters for enhanced graphene synthesis.

Keyword-graphene; electrochemical exfoliation; functional group; surface morphology; power

I. INTRODUCTION

Graphite is distinguished by its layered composition, with C atoms in each layer linked by covalent bonds and adjacent layers held by weak Van der Waals forces [1]. It exhibits thermal resilience, remaining stable up to 3825 °C before sublimation, and demonstrates exceptional electrical and thermal conduction properties [2]. The versatility of graphite is evident in diverse applications, from its use as an electrode in lithium-ion batteries to its employment in trolleybus current collectors [3, 4]. Graphite-derived nanomaterials, particularly graphene, have garnered significant interest from electrochemists due to their characteristics [5]. Graphene, a single-layer C structure in a honeycomb pattern formed through sp^2 hybridization, has become a point of extensive research [6-8]. Its attributes include superior electrical conductivity, vast surface area, chemical stability, and high capacitance [9, 10]. These properties make graphene promising for electrochemical applications [2]. Graphene also shows potential in developing flexible supercapacitors, lithium-ion batteries, corrosion-resistant coatings, and it is microwave absorbant [11-14].

The graphene synthesis methods are classified into top-down and bottom-up approaches. The top-down techniques include chemical exfoliation, liquid-phase exfoliation, arc-discharge method, ball milling exfoliation, and anodic electrochemical exfoliation [15-19]. The bottom-up strategies comprise epitaxial growth, chemical vapor deposition, and electric discharge [20, 21]. The top-down methods offer cost-effectiveness and simplicity, involving the fragmentation of graphite precursors into nano-sized graphene layers [19]. The bottom-up approaches typically require sophisticated equipment and high-temperature processes using costly transition metal ions [19, 21]. Electrochemical exfoliation, a top-down method, stands out for its simplicity, efficiency, environmental friendliness, and capacity for the large-scale production of high-quality graphene [19, 22-24]. This technique relies on the application of electrical potential to facilitate the ion intercalation between graphite layers. The expansion of space between layers facilitates the separation of graphite into single sheets of graphene [25, 26].

It has been demonstrated that current is a critical factor influencing the electrochemical exfoliation process and the resultant graphene's quantity and quality. In this process, an increase in current corresponds to a higher concentration of anions attracted to the anode. This phenomenon subsequently impacts the oxidation process, leading to enhanced intercalation. The interplay between these factors underscores the importance of current control in graphene production via electrochemical exfoliation [27]. In addition, the potential and duration of exfoliation affect graphene yield, while elevated voltage levels lead to an increased graphene production [28]. Applying high voltage during exfoliation increases the O content [29, 30]. This voltage shift causes aggressive destruction to exfoliation, increasing defect density, and ultimately lower quality [28, 31]. The high defect density and O content contribute to graphene quality degradation [32]. Moreover, electric power will demonstrate effects comparable to the voltage and current throughout the exfoliation process.

Previous studies have not thoroughly examined the specific role of power in the electrochemical exfoliation process. The present research seeks to clarify how power influences the quantity and quality of graphene by adjusting the voltage, current, and time parameters. The current work enhances the understanding of the electrochemical exfoliation process and provides valuable insights into optimizing power variables for improved graphene synthesis.

II. METHODOLOGY

This experiment examines the influence of power parameters, specifically voltage and current, on the electrochemical exfoliation of the graphite for graphene synthesis. Furthermore, raw materials, including graphite rod (diameter of 0.9 cm), distilled water, and ammonium sulfate (NH_2SO_4) electrolyte, are utilized for this study. In addition, electrochemical exfoliation is employed using a 0.1 M ammonium sulfate (NH_2SO_4) solution, with graphite rods functioning as both cathodes and anodes for three power settings: 70 W, 84 W, and 98 W. Analyzing the power dynamics is proven to be crucial for large-scale graphene production, as higher power levels are associated with increased graphene mass.

The electrolyte solution is prepared by dissolving NH_2SO_4 powder in distilled water to achieve a 0.1 M concentration, resulting in a homogeneous mixture [33]. Two precisely weighed graphite rods are immersed in the ammonium sulfate electrolyte and connected to DC power sources, serving as anodes and cathodes. The exfoliation process employes specific voltage settings and varied exposure times, enabling a systematic evaluation of their impact on the exfoliation efficiency. Current fluctuations, indicative of exfoliation dynamics, are carefully monitored throughout the procedure.

The applied voltage encourages the ions in the electrolyte to intercalate into the graphite electrode. This can increase the distance between the graphite layers [34]. Water molecules and sulphate ions migrate to the interstitial areas of graphite and create bubbles that separate adjacent sheets [34, 35]. This process induced a structural transformation in the graphite, culminating in the formation of graphene layers. Subsequently, the graphene is cleaned thoroughly with ethanol and centrifugation for 20 min, a process repeated multiple times. This procedure aimed to eliminate any remaining contaminants or impurities that could potentially affect the graphene. Following this, the purified graphene is preserved in distilled water to facilitate future analysis and application.

The characterization process, including the observed morphology and composition of graphene by SEM-EDX JEOL Benchtop SEM JCM 7000. The surface chemistry was analyzed by FTIR type Shimadzu IR Spirit, in a wavelength of 400-4.000 cm^{-1}, having determined the bonding of functional groups. The crystal structure was analyzed through X-Ray Diffractometer (XRD) Bruker D8 Advance (with 2θ was 10°-90°). Defect analysis of structure C was performed by Raman spectrometry.

III. RESULTS AND DISCUSSION

This study examined the influence of applied power on the electrochemical exfoliation of graphite in graphene synthesis. Current and voltage measurements are recorded throughout the exfoliation process. The current-voltage relationship plays a critical role in graphene production, as it affects both the qualitative and quantitative aspects of the resulting graphene. Table I illustrates the correlation between the voltage and the duration required to attain the optimal peak during electrochemical exfoliation. Higher voltages corresponded to increased optimal peak currents. This pattern deviated to 14 V. Moreover, while a precise relationship is not established, the applied voltages influence the necessary time for graphene to achieve the optimal current peak.

TABLE I. VOLTAGES AND DURATION CORRELATION

Voltage (V)	Optimal peak current (A)	Times (min)
10	3.22	73
11	4.81	32
12	6.39	47
13	7	24
14	6.4	28
15	8.54	17

In addition, the current flow on the graphite surface is observed through the tube blanket surface area equation. The current flowing per unit surface area of the graphite rod is 0.43 A/cm^2. This current results from the intercalation of anions on the graphite rod surfaces.

To examine the influence of the power input on the graphene mass production, an experimental investigation is conducted. The experiment explores the interrelationship between the mass yield, applied voltage, and current measurements over a 40-min duration, as illustrated in Figure 1. The experiment employed voltage levels of 10 V, 12 V, and 14 V, with corresponding power outputs of 70 W, 84 W, and 98 W. Figure 1a reveals a direct relationship between the magnitude of the applied voltage and the generated power. The data indicate that elevating the voltage leads to an increase in the power output.

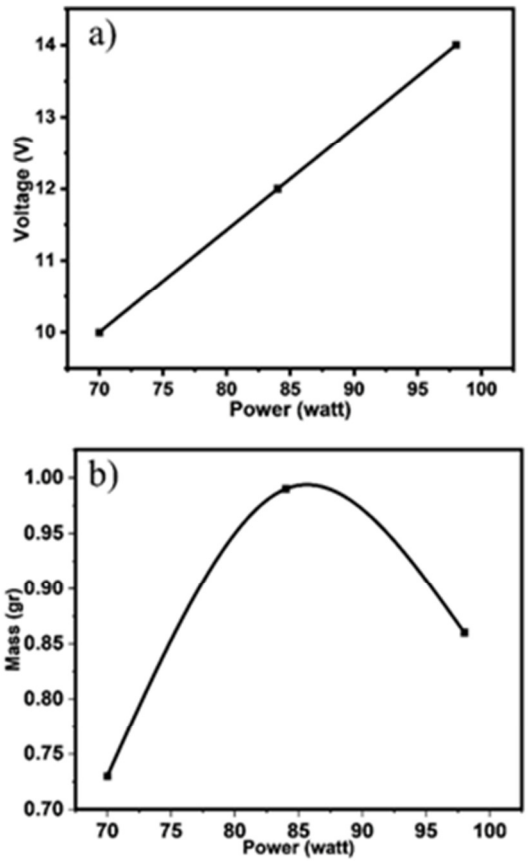

Fig. 1. Relatiosnhip of: (a) voltage against power, (b) mass against power.

Meanwhile, Figure 1b displays that an increase of graphene mass leads to an increase in power. For 70 W, the mass of graphene is 0.73 gr. Subsequently, the optimal conditions for maximizing graphene production efficiency are described by a mass of 0.99 gr and a power of 84 W. Furthermore, understanding the relationship between the power and mass provides improved control over the manufacturing process, potentially leading to more cost-effective and scalable approaches of graphene.

Moreover, the power-time relationship during graphene exfoliation over 120 min is investigated, as illustrated in Figure 2. Initially, in Figure 2a the baseline power is 50.4 W at 10 min, and the power continuously increases over time. However, beyond the 120 min point, the power drastically decreases to 36 W, as indicated in Table II.

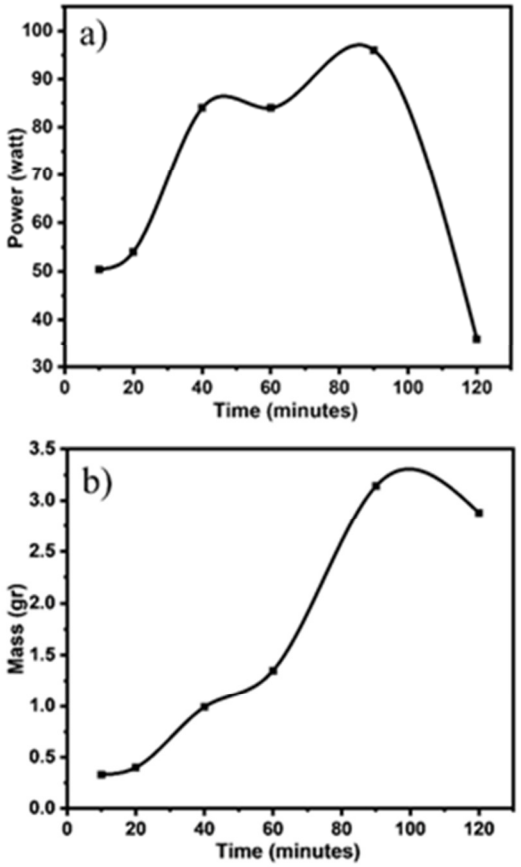

Fig. 2. Relatiosnhip of: (a) power against time, (b) mass against time.

This trend, evidenced in Table II, suggests an initial boost in power with prolonged experimentation, followed by an optimal peak at 90 min. The decrease in the power output after 90 min in this experiment can be attributed to the fact that the surface of the graphite rod was decreased.

TABLE II. THE RELATIONSHIP OF POWER AGAISNT TIME

Power (W)	Times (min)
50.4	10
54.0	20
84.0	40
84.0	60
96.0	90
36.0	120

Under continuous electrochemical exfoliation, the graphite rod's surface undergoes constant delamination, leading to a reduction in its surface area. Consequently, the current per area flowing in the graphite rod diminished, leading to decreases power, as depicted in Table II.

To analyze the surface morphology, SEM characterization is utilized for a detailed examination of the topography and composition of the particulate matter within the samples. SEM images of graphite and graphene, magnified 2,500 times, are presented in Figure 3. The graphene sample is produced by subjecting a graphite rod to an electrochemical exfoliation process lasting 40 min.

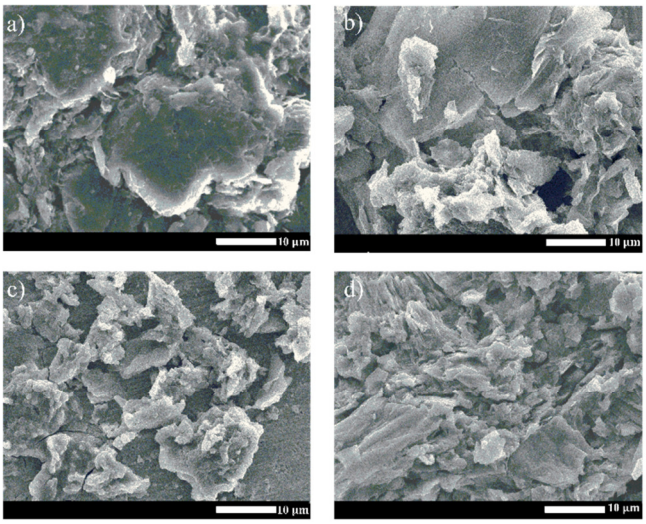

Fig. 3. SEM images of: (a) graphite, (b) graphene 70 W (G70), (c) graphene 84 W (G84), and (d) graphene 98 W (G98).

The electrochemical exfoliation process facilitates the conversion of graphite to graphene. This transformation is characterized by the detachment of nanocarbon sheets from the original graphite structure [36]. During exfoliation, the graphite edges expand leading to the separation and delamination of the graphite lattice into graphene layers [37].

Using the ImageJ softeare the size of the graphite particle materials is observed. The average particle sizes of graphite, G70, G84, and G98 are 14.8 µm, 13.87 µm, 10.40 µm, and 8.85 µm, respectively. The G70 sample exhibited a more pronounced and consistent layering compared to other variations. In contrast, G98 displayed a more crumpled and disorganized surface morphology. These observations suggest that increasing the power levels may compromise the structural integrity of graphene. Based on these measurements, the increase in power will decrease the particle material size. This indicates that the effect of destruction exfoliation is greater at high power. An EDX analysis, presented in Table III, provided insights into the elemental composition of both the graphite and graphene materials.

TABLE III. GRAPHITE AND GRAPHENE EDX RESUTLS

Element	Graphite (at%)	G70 (at%)	G84 (at%)	G98 (at%)
C	100.00±11.54	79.62±4.90	79.23±3.19	47.45±8.40
O	-	14.66±4.33	8.50±1.80	34.67±8.87
Fe	-	0.22±0.32	-	2.82±1.89
Cu	-	5.50±2.08	-	15.07±6.16
Ni	-	-	11.88±1.54	-

The graphite rod comprised 100% C. Conversely, samples G70, G84, and G98 demonstrated diverse elemental profiles, including C, O, copper (Cu), and iron (Fe). The C component originated from graphite. Table III depicts C concentrations of 79.62 at%, 79.23 at%, and 47.45 at% for G70, G84, and G98, respectively. A negative correlation is observed between the power input and C content. The O presence indicated oxidation during electrochemical exfoliation [38]. The O levels are measured at 14.66 at% for G70, 8.50 at% for G84, and 34.67 at% for G98.

The highest O concentration is detected in G98, corresponding to the maximum power input. This phenomenon is attributed to the accelerated reactions and enhanced oxidation processes at elevated power levels. Fe and nickel are identified as contaminants. In contrast, the Cu content is linked to the Cu foil utilized in the graphene sample preparation because of the liquid graphene sample coating onto the surface of the Cu foil. To avoid such a contamination, the sample form can be changed from liquid to powder. For the current study, contaminant Cu does not affect the mass of graphene.

Additionally, FTIR is employed to examine the functional groups present in graphite and graphene. The analysis spanned from 4,000 to 550 cm^{-1} and is performed under standard room temperature conditions. Figure 4 illustrates the resulting FTIR spectra, offering insights into the sample molecular vibrations and chemical bonding characteristics.

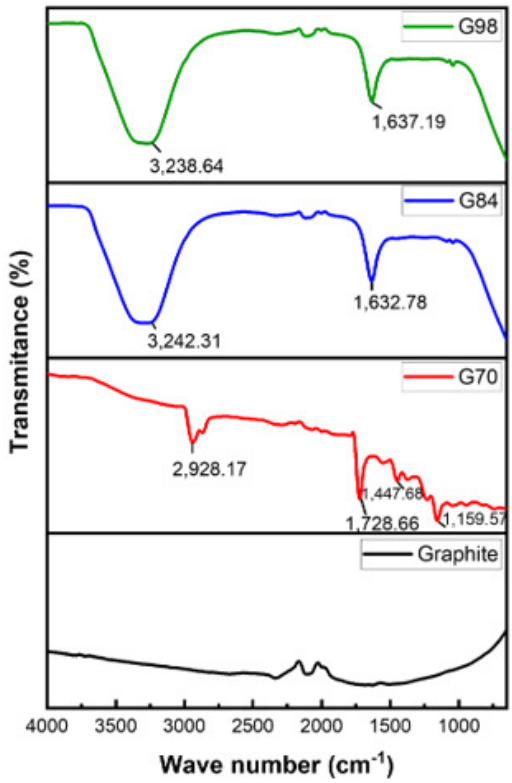

Fig. 4. FTIR spectra of graphite and graphene.

Based on the grouping of functional groups, as portrayed in Figure 4, it can be observed that graphite rods do not have absorption peaks. G70 has an absorption peak of 2,928.17 cm^{-1}, which is a functional C-H group, 1,728.66 cm^{-1} showed the C=O functional group, and 1,446.25 cm^{-1} and 1,159.57 cm^{-1} showed O-H bond. G84 has a strong absorption peak of 3,242.31 cm^{-1} allocated to O-H and the absorption peak on the C=C bond appeared at 1,632.78 cm^{-1}. Meanwhile, G98 has a strong absorption peak at 3,238.64 cm^{-1} that presented an O-H bond, and at 1,637.19 cm^{-1} is stretching of C=C bond [39, 40]. The sharp peak is a C=O bond that exists on G70, while G84 and G98 have sharp peaks of O-H bonds. In addition, the C-H peaks at G84 and G98 are reduced. This occurs due to the oxidation process [41]. G84 and G98 utilized higher power than G70, so that the oxidation process is also high. The oxidation occurs due to the reaction between the exfoliated graphene layers and the oxygen produced from the electrolyte [42].

The structure crystal of graphene was analyzed using XRD, as shown in Figure 5. The XRD testing is carried out with 2θ between 10 ° and 90 °. Figure 5 illustrates the XRD of graphite and graphene. Regarding the graphite, a sharp peak in 26.44 ° is observed, which corresponds to the (002) plane, with spacing being 0.337 nm. Additionally, the other peaks are at 44.3 ° and 54.4 °, which correspond to (101) and (004), respectively. However, graphene has a sharp peak in 26.59 °, which corresponds to (002) plane, with spacing being 0.336 nm. Other peaks with low intensity consist of 44.6 ° and 54.7 °, which correspond to (101) and (004) plane, respectively [25]. The Full Width at Half Maximum (FWHM) values are 0.47 for graphite and 0.51 for graphene. The graphite and graphene peaks have a similar shape due to their similar nature, and therefore the diffraction peaks become narrower [43]. During the XRD analysis, the peaks appearing in the material belong to graphene and the oxidation process is not detected. When detected, the corresponding peak appears between 10 ° and 13 ° and the material becomes graphene oxide [44].

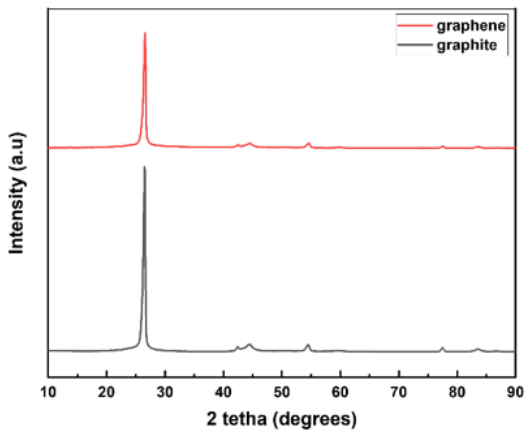

Fig. 5. XRD pattern of graphite and graphene.

Raman spectroscopy is utilized to analyze material defects. As depicted in Figure 6, the D-band exhibits a lower intensity compared to the G-band, while also the 2D band appears to have low intensity. The Raman spectrum of the graphite rod shows D, G, and 2D bands at 1343 cm^{-1}, 1574 cm^{-1}, and 2703

cm^{-1}, respectively. Similarly, the graphene spectrum presents D, G, and 2D bands at 1343 cm^{-1}, 1577 cm^{-1}, and 2709 cm^{-1}, respectively. The D band is associated with defects in graphene, while the G-band corresponds to C sp2 hybridization in graphite. The 2D band reflects variations in graphene layer thickness and two-phonon scattering [26, 35]. The low intensity of the 2D peak, evidenced in Figure 6, indicates a reduced surface area of the sp2 domain following the exfoliation process [45]. The G band demonstrates the highest peak intensity for both materials; however, the graphene G band exhibits a sharper intensity compared to that of the graphite, suggesting chemical doping [46]. The intensity ratio (I_D/I_G) for graphite and graphene is 0.83 and 0.77, respectively, indicating a lower defect density in graphene compared to graphite.

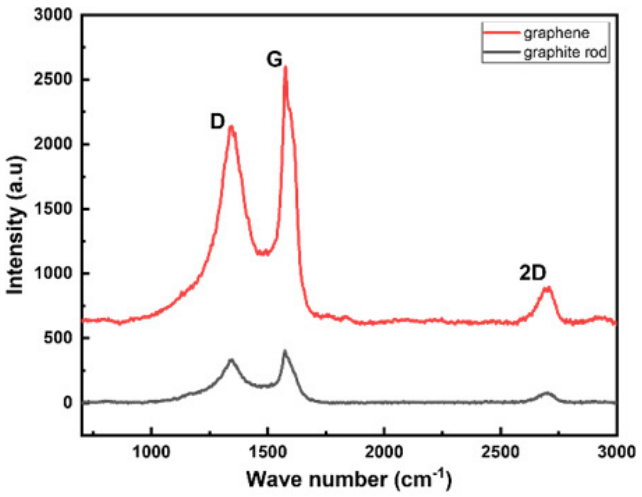

Fig. 6. Raman spectroscopy of graphite rod and graphene.

The present study enhances the comprehension of the electrochemical exfoliation process and establishes practical protocols for optimizing power parameters in graphene synthesis. The ongoing investigation of innovative materials and applications contributes to the expansion of knowledge in the nanomaterials domain, thereby facilitating future progress in graphene-based technological advancements.

IV. CONCLUSIONS

In this study, the electrochemical exfoliation process for synthesizing graphene is investigated with varying applied powers (70 W, 84 W, and 98 W). The Scanning Electron Microscope (SEM) analysis confirmed a graphene sheet formation under all power conditions, with the most wrinkles for grapheme observed at 98 W (G98). The Energy Dispersive X-Ray (EDX) analysis highlighted the highest Carbon (C) content in exfoliated graphite for graphene at 70 W (G70), decreasing for graphene at 84 W (G84) and G98. The most Oxygen (O) content appeared for G98. Increasing the power reduced C and increased oxidation due to the O content. The Fourier Transform Infrared (FTIR) revealed absorption peaks between 1,159.57-3,242.31 cm^{-1}, with a prominent peak at 1,728.66 cm^{-1} corresponding to C=O bonds for G70. Sharp O=H peaks at 3,242.31 cm^{-1} and 3,238.64 cm^{-1} appeared for G84 and G98.

Finally, the experimental investigation exhibited a direct correlation between the power input parameters and graphene production yield, with higher power levels resulting in an increased graphene output. However, the study also indicated that excessive power negatively impacts the exfoliation process efficiency, identifying 70 W as the optimal power setting for the graphene synthesis. These findings significantly contribute to understanding the electrochemical exfoliation mechanism and provide valuable insights for refining the power parameters in graphene manufacturing processes.

ACKNOWLEDGEMENT

This research was funded by UNS Research Grant (Penelitian Hibah Grup Riset) with contract number 228/UN27.22/PT.01.03/2024. The authors acknowledge the facilities, scientific and technical support from AdvancedCharacterization Laboratories Serpong, National Research and Innovation Agency through E-Layanan Sains, Badan Riset dan Inovasi Nasional.

REFERENCES

[1] A. A. Moosa, Z. H. Mahdi, and M. A. Mutar, "Preparation of Graphene Oxide from Expanded Graphite at Different Microwave Heating Times," *Journal of Engineering and Technological Sciences*, vol. 53, no. 3, pp. 210305–210305, Jun. 2021, https://doi.org/10.5614/j.eng.technol.sci.2021.53.3.5.

[2] A. Ambrosi, C. K. Chua, A. Bonanni, and M. Pumera, "Electrochemistry of Graphene and Related Materials," *Chemical Reviews*, vol. 114, no. 14, pp. 7150–7188, Jun. 2014, https://doi.org/10.1021/cr500023c.

[3] F. Jeschull *et al.*, "Graphite Particle-Size Induced Morphological and Performance Changes of Graphite–Silicon Electrodes," *Journal of The Electrochemical Society*, vol. 167, no. 10, Mar. 2020, Art. no. 100535, https://doi.org/10.1149/1945-7111/ab9b9a.

[4] R. Mirea, "Advanced Graphite/Metal Composite Materials for High Voltage Automotive Applications," *Engineering, Technology & Applied Science Research*, vol. 14, no. 5, pp. 17302–17307, Oct. 2024, https://doi.org/10.48084/etasr.7988.

[5] D. A. C. Brownson, G. C. Smith, and C. E. Banks, "Graphene oxide electrochemistry: the electrochemistry of graphene oxide modified electrodes reveals coverage dependent beneficial electrocatalysis," *Royal Society Open Science*, vol. 4, no. 11, Nov. 2017, Art. no. 171128, https://doi.org/10.1098/rsos.171128.

[6] K. Kakaei, "One-pot electrochemical synthesis of graphene by the exfoliation of graphite powder in sodium dodecyl sulfate and its decoration with platinum nanoparticles for methanol oxidation," *Carbon*, vol. 51, pp. 195–201, Jan. 2013, https://doi.org/10.1016/j.carbon.2012.08.028.

[7] R. B. Kohakade, E. S. Kumar, R. W. Gaikwad, S. Raghu, and R. A. Kalaivani, "Electrochemical Surface Oxidation of Graphite Electrode and Its Superior Sensitive Platform For Electrochemical Sensors," *Rasayan Journal of Chemistry*, vol. 10, no. 4, pp. 1151–1158, 2017, http://dx.doi.org/10.7324/RJC.2017.1041881.

[8] J. Mei *et al.*, "Process regulation of the electrochemical exfoliation for graphene production with graphite powder as starting materials," *Journal of Materials Science*, vol. 58, no. 22, pp. 9116–9129, May 2023, https://doi.org/10.1007/s10853-023-08601-5.

[9] E. Yoo, J. Kim, E. Hosono, H. Zhou, T. Kudo, and I. Honma, "Large Reversible Li Storage of Graphene Nanosheet Families for Use in Rechargeable Lithium Ion Batteries," *Nano Letters*, vol. 8, no. 8, pp. 2277–2282, Jun. 2008, https://doi.org/10.1021/nl800957b.

[10] D. Lee and J. Seo, "Layer-by-layer-stacked graphene/graphene-island supercapacitor," *AIP Advances*, vol. 10, no. 5, May 2020, Art. no. 055202, https://doi.org/10.1063/5.0007887.

[11] N. P. Sari, D. Dutta, A. Jamaluddin, J.-K. Chang, and C.-Y. Su, "Controlled multimodal hierarchically porous electrode self-assembly of electrochemically exfoliated graphene for fully solid-state flexible supercapacitor," *Physical Chemistry Chemical Physics*, vol. 19, no. 45, pp. 30381–30392, Nov. 2017, https://doi.org/10.1039/C7CP05799G.

[12] A. Jamaluddin, B. Umesh, F. Chen, J.-K. Chang, and C.-Y. Su, "Facile synthesis of core–shell structured Si@graphene balls as a high-performance anode for lithium-ion batteries," *Nanoscale*, vol. 12, no. 17, pp. 9616–9627, May 2020, https://doi.org/10.1039/D0NR01346C.

[13] M. U. Arshad *et al.*, "Multi-functionalized fluorinated graphene composite coating for achieving durable electronics: Ultralow corrosion rate and high electrical insulating passivation," *Carbon*, vol. 195, pp. 141–153, Apr. 2022, https://doi.org/10.1016/j.carbon.2022.04.004.

[14] A. Peyravi, F. Ahmadijokani, M. Arjmand, and Z. Hashisho, "Graphene oxide enhances thermal stability and microwave absorption/regeneration of a porous polymer," *Journal of Hazardous Materials*, vol. 433, p. 128792, Jul. 2022, https://doi.org/10.1016/j.jhazmat.2022.128792.

[15] M. Cai, D. Thorpe, D. H. Adamson, and H. C. Schniepp, "Methods of graphite exfoliation," *Journal of Materials Chemistry*, vol. 22, no. 48, pp. 24992–25002, Nov. 2012, https://doi.org/10.1039/C2JM34517J.

[16] Y. Yang, F. Lu, Z. Zhou, W. Song, Q. Chen, and X. Ji, "Electrochemically cathodic exfoliation of graphene sheets in room temperature ionic liquids N-butyl, methylpyrrolidinium bis(trifluoromethylsulfonyl)imide and their electrochemical properties," *Electrochimica Acta*, vol. 113, pp. 9–16, Sep. 2013, https://doi.org/10.1016/j.electacta.2013.09.031.

[17] M. Yusuf, M. Kumar, M. A. Khan, M. Sillanpää, and H. Arafat, "A review on exfoliation, characterization, environmental and energy applications of graphene and graphene-based composites," *Advances in Colloid and Interface Science*, vol. 273, Oct. 2019, Art. no. 102036, https://doi.org/10.1016/j.cis.2019.102036.

[18] L. Saikam, P. Arthi, B. Senthil, and M. Shanmugam, "A review on exfoliated graphite: Synthesis and applications," *Inorganic Chemistry Communications*, vol. 152, Apr. 2023, Art. no. 110685, https://doi.org/10.1016/j.inoche.2023.110685.

[19] A. Agrawal, "Top-down strategies for achieving high-quality graphene: Recent advancements," *Journal of Industrial and Engineering Chemistry*, vol. 142, pp. 103–126, Dec. 2024, https://doi.org/10.1016/j.jiec.2024.07.053.

[20] Y. Yang, F. Lu, Z. Zhou, W. Song, Q. Chen, and X. Ji, "Electrochemically cathodic exfoliation of graphene sheets in room temperature ionic liquids N-butyl, methylpyrrolidinium bis(trifluoromethylsulfonyl)imide and their electrochemical properties," *Electrochimica Acta*, vol. 113, pp. 9–16, Nov. 2013, https://doi.org/10.1016/j.electacta.2013.09.031.

[21] A. Gutiérrez-Cruz, A. R. Ruiz-Hernández, J. F. Vega-Clemente, D. G. Luna-Gazcón, and J. Campos-Delgado, "A review of top-down and bottom-up synthesis methods for the production of graphene, graphene oxide and reduced graphene oxide," *Journal of Materials Science*, vol. 57, no. 31, pp. 14543–14578, Aug. 2022, https://doi.org/10.1007/s10853-022-07514-z.

[22] K. Parvez *et al.*, "Exfoliation of Graphite into Graphene in Aqueous Solutions of Inorganic Salts," *Journal of the American Chemical Society*, vol. 136, no. 16, pp. 6083–6091, Mar. 2014, https://doi.org/10.1021/ja5017156.

[23] Y. Zhang, Y. Xu, Y. Niu, W. Hou, and R. Liu, "Highly efficient dual-electrode exfoliation of graphite into high-quality graphene via square-wave alternating currents," *Chemical Engineering Journal*, vol. 456, Dec. 2022, Art. no. 140977, https://doi.org/10.1016/j.cej.2022.140977.

[24] D. Ehjeij *et al.*, "Electrochemical Exfoliation of Graphene and Formation of its Copolyamide 6/66 Nanocomposites by Wet Phase Inversion and Injection Molding," *Macromolecular Chemistry and Physics*, vol. 226, no. 1, Oct. 2025, Art. no. 2400320, https://doi.org/10.1002/macp.202400320.

[25] X. Zhao *et al.*, "Electrochemical exfoliation of graphene as an anode material for ultra-long cycle lithium ion batteries," *Journal of Physics and Chemistry of Solids*, vol. 139, Dec. 2019, Art. no. 109301, https://doi.org/10.1016/j.jpcs.2019.109301.

[26] T. N. J. I. Edison *et al.*, "Electrochemically exfoliated graphene sheets as electrode material for aqueous symmetric supercapacitors," *Surface and Coatings Technology*, vol. 416, Apr. 2021, Art. no. 127150, https://doi.org/10.1016/j.surfcoat.2021.127150.

[27] W.-W. Liu and A. Aziz, "Review on the Effects of Electrochemical Exfoliation Parameters on the Yield of Graphene Oxide," *ACS Omega*, vol. 7, no. 38, pp. 33719–33731, Sep. 2022, https://doi.org/10.1021/acsomega.2c04099.

[28] P. K. M. K, S. Shanthini, and C. Srivastava, "Electrochemical exfoliation of graphite for producing graphene using saccharin," *RSC Advances*, vol. 5, no. 66, pp. 53865–53869, Jun. 2015, https://doi.org/10.1039/C5RA07846F.

[29] S. Tian *et al.*, "One-step fast electrochemical fabrication of water-dispersible graphene," *Carbon*, vol. 111, pp. 617–621, Oct. 2016, https://doi.org/10.1016/j.carbon.2016.10.044.

[30] M. Coroș *et al.*, "Simple and cost-effective synthesis of graphene by electrochemical exfoliation of graphite rods," *RSC Advances*, vol. 6, no. 4, pp. 2651–2661, Jan. 2016, https://doi.org/10.1039/C5RA19277C.

[31] A. Taheri Najafabadi and E. Gyenge, "Synergistic production of graphene microsheets by simultaneous anodic and cathodic electro-exfoliation of graphitic electrodes in aprotic ionic liquids," *Carbon*, vol. 84, pp. 449–459, Dec. 2014, https://doi.org/10.1016/j.carbon.2014.12.041.

[32] F. Alabdo, W. Alahmad, U. Pengsomjit, M. Halabi, P. Varanusupakul, and C. Kraiya, "An environmentally friendly and simple method for producing multi-layer exfoliated graphene in mass production from pencil graphite and its utilization for removing cadmium from an aqueous medium," *Carbon Letters*, vol. 33, no. 2, pp. 455–465, Nov. 2022, https://doi.org/10.1007/s42823-022-00435-6.

[33] N. N. Aida, M. Ikhsanudin, A. Jamaludin, A. Nur'aini, E. L. Septiani, and H. Widiyandari, "Synthesis of Graphene from Pencils Graphite Via Electrochemical Exfoliation Method as a Cu-Foil Coating on the Anode-Free Lithium-Ion Battery," *ALCHEMY Jurnal Penelitian Kimia*, vol. 20, no. 1, pp. 31–37, Mar. 2024, https://doi.org/10.20961/alchemy.20.1.74620.31-37.

[34] T. C. Achee *et al.*, "High-yield scalable graphene nanosheet production from compressed graphite using electrochemical exfoliation," *Scientific Reports*, vol. 8, no. 1, Sep. 2018, Art. no. 14525, https://doi.org/10.1038/s41598-018-32741-3.

[35] A. A. Muhsan and K. Lafdi, "Numerical study of the electrochemical exfoliation of graphite," *SN Applied Sciences*, vol. 1, no. 3, Feb. 2019, Art. no. 276, https://doi.org/10.1007/s42452-019-0296-8.

[36] S. Vadivel, W. Tejangkura, and M. Sawangphruk, "Graphite/Graphene Composites from the Recovered Spent Zn/Carbon Primary Cell for the High-Performance Anode of Lithium-Ion Batteries," *ACS Omega*, vol. 5, no. 25, pp. 15240–15246, Jun. 2020, https://doi.org/10.1021/acsomega.0c01270.

[37] S. H. Ilias, J. A. Murshidi, and K. K. Ying, "Effect of electrolyte concentration on the synthesis of graphene by electrochemical exfoliation process," *IOP Conference Series: Materials Science and Engineering*, vol. 1106, no. 1, Nov. 2021, Art. no. 012013, https://doi.org/10.1088/1757-899X/1106/1/012013.

[38] R. Patil, H. Patel, S. B. Pillai, P. K. Jha, P. Bahadur, and S. Tiwari, "Influence of surface oxygen clusters upon molecular stacking of paclitaxel over graphene oxide sheets," *Materials Science & Engineering. C, Materials for Biological Applications*, vol. 116, Jun. 2020, Art. no. 111232, https://doi.org/10.1016/j.msec.2020.111232.

[39] V. Țucureanu, Matei ,Alina, and A. M. and Avram, "FTIR Spectroscopy for Carbon Family Study," *Critical Reviews in Analytical Chemistry*, vol. 46, no. 6, pp. 502–520, Jun. 2016, https://doi.org/10.1080/10408347.2016.1157013.

[40] S. Sedaghat, M. M. Ahadian, M. Jafarian, and S. Hatamie, "Model Fuel Deep Desulfurization Using Modified 3D Graphenic Adsorbents: Isotherm, Kinetic, and Thermodynamic Study," *Industrial & Engineering Chemistry Research*, vol. 58, no. 24, pp. 10341–10351, May 2019, https://doi.org/10.1021/acs.iecr.9b00250.

[41] Y. Chen *et al.*, "Updated understandings on coke formation during the inferior heavy oil in-situ combustion process: A combined FTIR, XPS, TG/DTG, and DSC study," *Sustainable Energy Technologies and Assessments*, vol. 65, Apr. 2024, Art. no. 103772, https://doi.org/10.1016/j.seta.2024.103772.

[42] M. Ostermann, L. Kalchgruber, J. Schodl, P. Lieberzeit, P. Bilotto, and M. Valtiner, "Tailoring the properties of graphene nanosheets during electrochemical exfoliation," *Carbon Trends*, vol. 18, Dec. 2024, Art. no. 100449, https://doi.org/10.1016/j.cartre.2024.100449.

[43] E. A. Ganash, G. A. Al-Jabarti, and R. M. Altuwirqi, "The synthesis of carbon-based nanomaterials by pulsed laser ablation in water," *Materials Research Express*, vol. 7, no. 1, Nov. 2019, Art. no. 015002, https://doi.org/10.1088/2053-1591/ab572b.

[44] S. Li, J. Zhang, M. Liu, R. Wang, and L. Wu, "Influence of polyethyleneimine functionalized graphene on tribological behavior of epoxy composite," *Polymer Bulletin*, vol. 78, no. 11, pp. 6493–6515, Oct. 2020, https://doi.org/10.1007/s00289-020-03439-2.

[45] M. Eredia *et al.*, "Morphology and Electronic Properties of Electrochemically Exfoliated Graphene," *The Journal of Physical Chemistry Letters*, vol. 8, no. 14, pp. 3347–3355, Jul. 2017, https://doi.org/10.1021/acs.jpclett.7b01301.

[46] A. C. Ferrari *et al.*, "Raman Spectrum of Graphene and Graphene Layers," *Physical Review Letters*, vol. 97, no. 18, Oct. 2006, Art. no. 187401, https://doi.org/10.1103/PhysRevLett.97.187401.